Efficient Algorithm for Unsteady Transonic Aerodynamics of Low-Aspect-Ratio Wings

Guru P. Guruswamy*
Informatics General Corporation, Palo Alto, California
and
Peter M. Goorjian*
NASA Ames Research Center, Moffett Field, California

An efficient coordinate transformation technique is presented for constructing grids for unsteady transonic aerodynamic computations for delta-type wings. The original shearing transformation yielded computations that were numerically unstable, and this paper discusses the sources of those instabilities. The new shearing transformation yields computations that are stable, fast, and accurate. Comparisons of those two methods are shown for the flow over the F5 wing that demonstrate the new stability. Also, comparisons are made with experimental data that demonstrate the accuracy of the new method. The computations were made by using a time-accurate, finite-difference, alternating-direction-implicit (ADI) algorithm for the transonic small-disturbance potential equation.

Introduction

THERE is a need both by aerodynamicists and aeroelasticians for efficient computational methods in the area of three-dimensional unsteady transonic aerodynamics for the design of aircraft in the transonic regime. Such methods are being developed in the area of computation fluid dynamics (CFD).[1] Methods based on the small-disturbance theory have already led to the development of successful production codes that are in use for aeroelastic applications.[2,3] Methods based on other theories, such as the full-potential theory, are still in the early stages of development[4] for three-dimensional calculations. Among small-disturbance codes, XTRAN3S[2] is being actively used for aerodynamic and aeroelastic applications.[2,5-8]

XTRAN3S is a three-dimensional, unsteady, transonic small-disturbance potential code based on a time-accurate, finite-difference method using an alternating-direction-implicit (ADI) scheme. This code can analyze general wing configurations and can conduct static and dynamic aeroelastic computations by simultaneously integrating the aerodynamic and structural equations of motion. XTRAN3S has so far been successfully applied to the aerodynamic and aeroelastic analysis of wings with high-aspect ratios, large-taper ratios, and small sweep angles, e. g., rectangular or transport-type wings.[2,5-8] From these studies it has been observed[6,7] that XTRAN3S requires 360-1200 time steps/cycle for rectangular and transport-type wings, respectively, to give stable, accurate, unsteady results. With a decrease in the aspect ratio and the taper ratio and an increase in the sweep angle, the number of time steps required per cycle increases.

Preliminary computations diverged when an attempt was made to obtain steady results for the F5 wing,[9] which has an aspect ratio of 2.98, a taper ratio of 0.31, and a leading-edge sweep of 32 deg. (These computations were made jointly with W. A. Sotamayer, Air Force Wright Aeronautical Laboratories). The code was unstable at feasible time-step sizes such as $\Delta t = 0.01$, and it was still unstable at a very small time-step size of $\Delta t = 0.001$. At this smaller time-step size, unsteady computations (if stable) would have required about 30,000 time steps/cycle at a reduced frequency of 0.2. These facts have imposed severe limitations on the practical applications of XTRAN3S. (Similar failures have been reported by other investigators.[8])

The main objective of this work was to investigate in detail the sources of numerical instabilities in the procedures used in XTRAN3S and to develop stable new procedures. From studies conducted on the basic procedures employed in the code, it was found that the shearing coordinate transformation used in XTRAN3S was a major source of instability. As a result, an alternate, modified shearing coordinate transformation has been developed. This new transformation gives stable and accurate results for cases that failed with the old transformation technique. These results were obtained at a time-step size that is ten times larger than the size at which the old method was unstable.

With the modified shearing-transformation procedure, steady and unsteady computations were made at $M = 0.80$, $M = 0.90$, and $M = 0.95$, and they were compared with wind tunnel experiments.[9]

Sources of Instability

XTRAN3S uses a modified small-disturbance equation.[10]

$$A\phi_{tt} + B\phi_{xt} = (E\phi_x + F\phi^2{}_x + G\phi_y^2)_x + (\phi_y + H\phi_x\phi_y)_y + (\phi_z)_z \tag{1}$$

where $A = M_\infty^2$, $B = 2M_\infty^2$, $E = (1 - M_\infty^2)$, $F = -(\frac{1}{2})(\gamma + 1)M_\infty^2$, $G = (\frac{1}{2})(\gamma - 3)M_\infty^2$, and $H = -(\gamma - 1)M_\infty^2$.

Equation (1), which is ideal for rectangular wings, can pose problems for swept tapered wings. The dependence of the solution on the wing leading-edge mesh spacing poses a problem when applied to swept tapered wings. Because of the large number of points required, it is impractical to maintain a sufficiently fine mesh spacing along the leading edge of a swept wing in a Cartesian coordinate system. An alternative approach was developed by Ballhaus and Bailey,[11] who used a shearing transformation to map a trapezoidal planform wing in the physical plane into a rectangle in the computational

Presented as Paper 84-0872 at the AIAA/ASME/ASCE/AHS 25th Structures, Structural Dynamics and Materials Conference, Palm Springs, Calif., May 14-16, 1984, received March 24, 1984; revision received Dec. 19, 1984. This paper is declared a work of the U.S. Government and therefore is in the public domain.

*Research Scientist. Member AIAA.

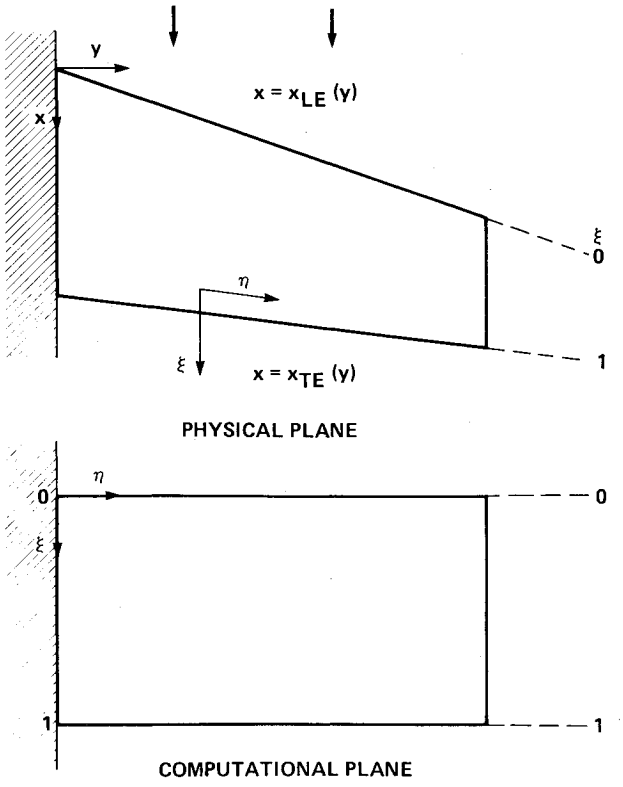

Fig. 1 Wing planform transformation.

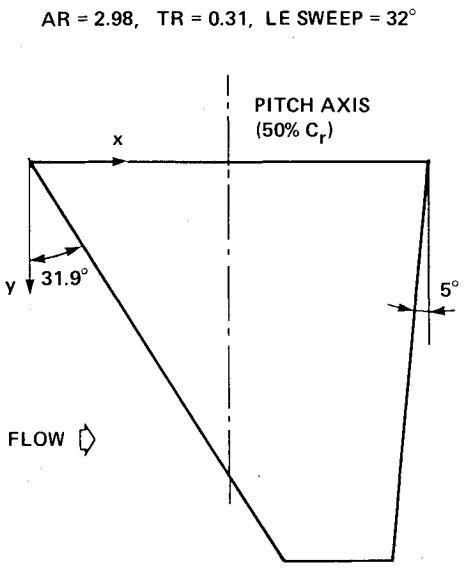

Fig. 2 Dimensions of the F5 wing.

plane as shown in Fig. 1, where

$$\xi(x,y)=\frac{x-x_{LE}(y)}{x_{TE}(y)-x_{LE}(y)}, \qquad \eta(y)=y, \qquad \zeta(z)=z \tag{2}$$

Use of this shearing transformation permits a more efficient distribution of mesh points. The leading and trailing edges lie on the coordinate lines $\xi=0$ and 1, respectively, and each span station ($\eta=$ constant) has the same number of chordwise mesh points on the wing surface. Thus, the complicating effect of geometry has been transferred from the boundary conditions to the governing equation. This shearing transformation was used in XTRAN3S throughout the flowfield.

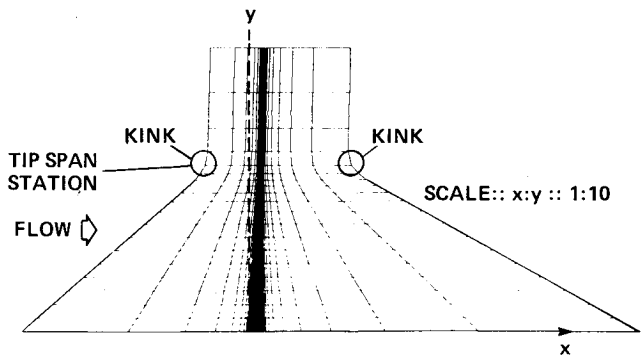

Fig. 3 Physical grid (64×20) in *x-y* plane from the conventional shearing transformation.

The conventional shearing-transformation Eq. (2) is simple and adequate for wings with high-aspect ratios, small sweeps, and large taper ratios.[2,6-8] Also, it was adequate for steady-state computations where the grid boundaries were located very close to the wing, approximately two to three chords from the wing edge. However, for unsteady computation on wings with low-aspect ratios, high sweeps, and small taper ratios (such as delta wings), use of this shearing transformation produces unstable calculations. For unsteady computations, in order to avoid boundary reflections, the grid boundaries need to be located far away from the wing edges. Since the transformation Eq. (2) is only a function of local chord, computational flow regions obtained by its use depend on the planform. For delta-type wings, Eq. (2) yields highly skewed flow regions and thus large discontinuous values for the metrics ξ_y near the upstream- and downstream-flow boundaries. The metric ξ_y appears as a coefficient of the cross derivatives in the governing equation—as seen later in Eq. (3)—after applying the transformation Eq. (2) to Eq. (1). Far-field grid boundaries are not aligned to the flow directions. Also in XTRAN3S, the cross derivatives have been differenced explicitly. These combined factors can make flow computations unstable (see the F5 wing).

Figure 2 shows the planform of the F5 wing, which has an aspect ratio of 2.98, a taper ratio of 0.31, and a leading-edge sweep angle of 31.92 deg. The computational flow region that was obtained by using the shearing-transformation Eq. (2) is shown in Fig. 3. From this figure, the large skewness of the grid lines, which causes large gradients for the metrics near the flow boundaries, can be observed. In fact, the scale in Fig. 3 is stretched 10 to 1 in the *y* (or vertical) direction. So the actual skewness is 10 times worse than shown. Also the kink (i.e., discontinuity) in the upstream boundary grid line is 10 times worse than shown. Figure 4a shows a plot of the metric value ξ_y vs *chord* for the root station for this shearing transformation. Figure 4b shows a corresponding plot of the metric value vs *span* along a grid line starting at a distance 15.6 chords from the leading edge of the root section. The downstream boundary is located 25 chords downstream at the root span station. From Fig. 4a, it is seen that ξ_y has a large value at the downstream boundary and, from Fig. 4b, ξ_y also changes value at the tip span location in a large discontinuous way. It is precisely at that location (the downstream boundary at the wing-tip span station) that numerical instabilities originate when Eq. (2) is used for calculations of flow over the F5 wing.

Using this grid, steady, transonic flow computations were unstable for a time-step size of $\Delta t=0.01$, which is 10 times smaller than that used for a stable calculation in a case for a rectangular wing.[6] However, fair steady-state results were obtained for subcritical flow at $M=0.8$ by using a small time step of $\Delta t=0.001$ and running the code for 2000 time steps. For the same time-step size of $\Delta t=0.001$, at $M=0.9$, where the flow was transonic, the calculations diverged. For most of the cases considered, the numerical instability started at the

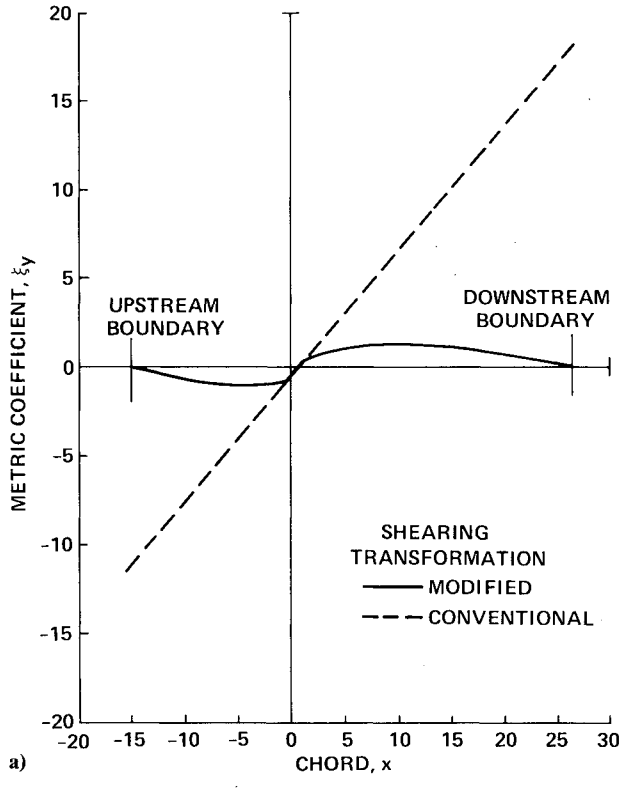

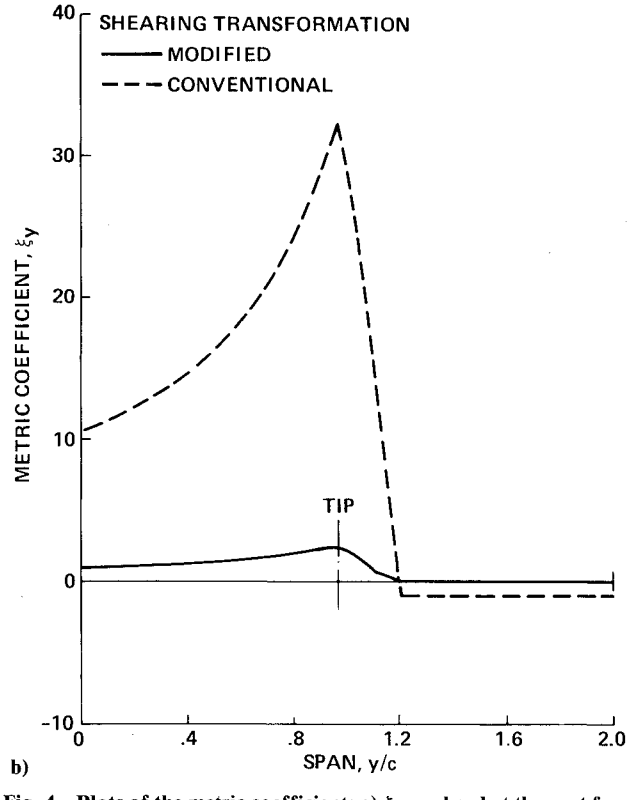

Fig. 4 Plots of the metric coefficient: a) ξ_y vs chord at the root from the two transformations; b) ξ_y vs span near downstream from the two transformations.

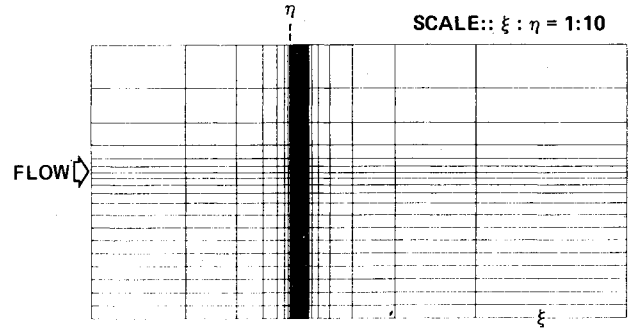

Fig. 5 Computational mesh (64×20) in $\xi-\eta$ plane.

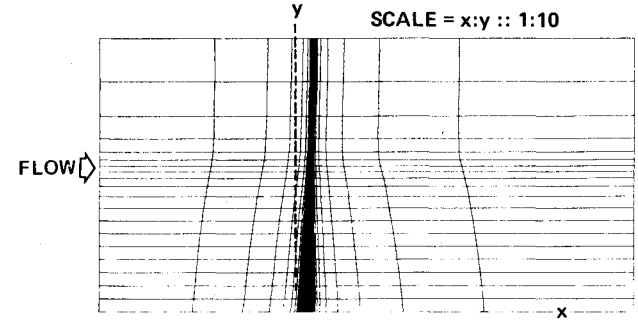

Fig. 6 Physical grid (64×20) in x-y plane by the modified shearing transformation.

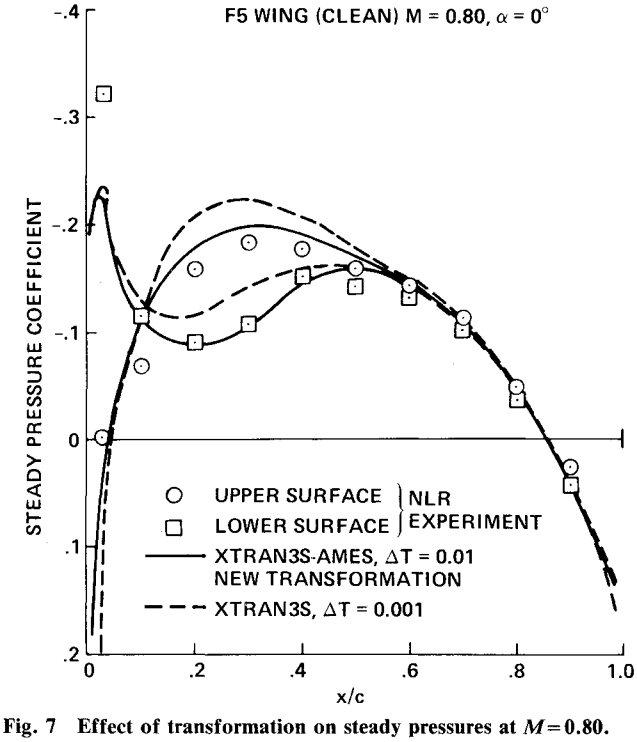

Fig. 7 Effect of transformation on steady pressures at $M=0.80$.

downstream boundary where the tip span station occurs. For comparison, the conventional shearing-transformation Eq. (2) gives stable results for transport-type wings, in which case there is no kink in the transformation. This leads to the conclusion that this feature of transformation is causing the numerical instability. As a result, this work presents an alternate transformation procedure that does not have the property of employing metrics that have large discontinuous values. This new transformation will yield stable calculations.

Modified Shearing Transformation

The main requirement that any transformation should satisfy for the finite-difference method used in XTRAN3S is that it should map any given wing to a rectangular wing (see Fig. 1). This condition is satisfied in the modified shearing

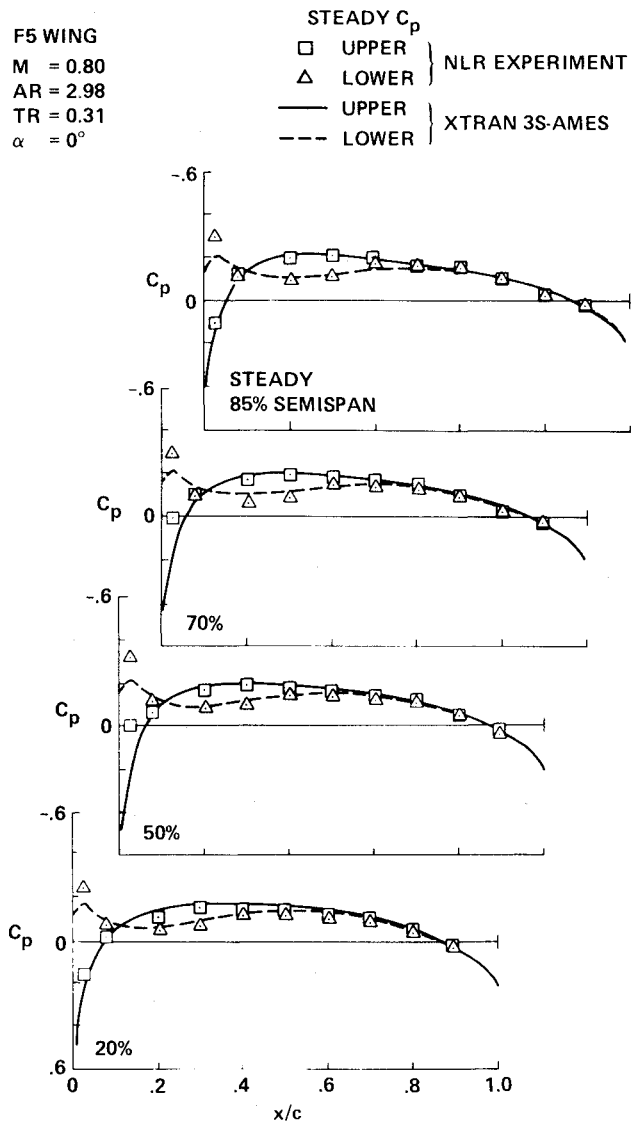

Fig. 8 Comparison of steady pressures between theory and experiment at $M=0.80$.

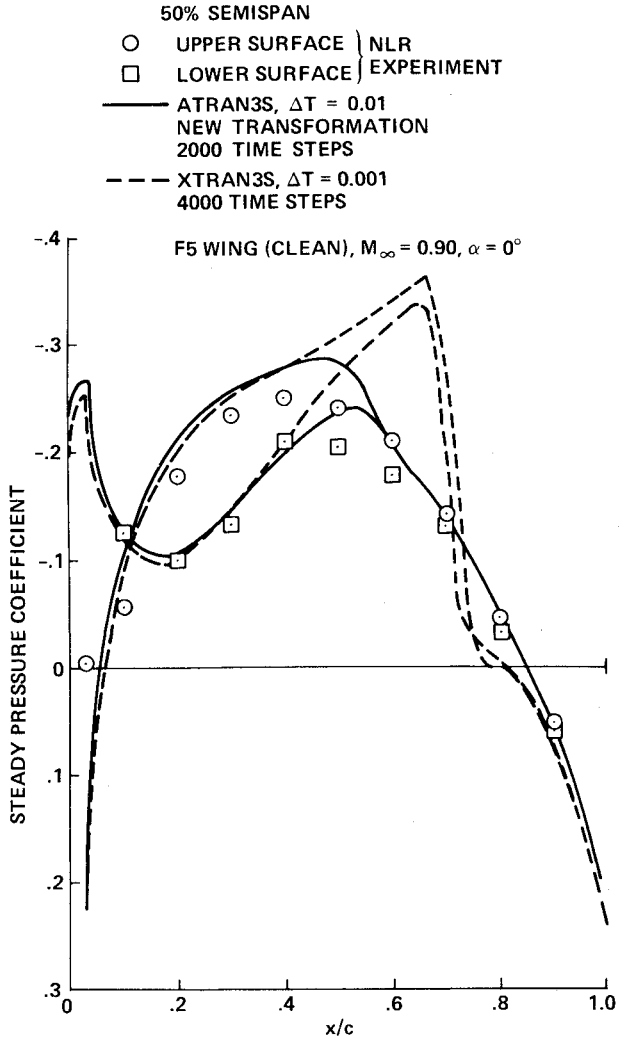

Fig. 9 Effect of transformation on steady pressures at $M=0.90$.

transformation by using the same conventional shearing transformation given by Eq. (2) in the region near the wing. Away from the wing, a new scheme is devised such that the grid lines have the following characteristics: 1) far-field boundaries are independent of the wing planform and aligned with respect to the freestream direction; 2) smooth first and second derivatives occur for values of the metric quantities, particularly near boundaries; 3) grid lines are clustered near the leading and trailing edges.

A good transformation that satisfies all the above criteria is shown in Figs. 5 and 6. The computational mesh in Fig. 5 is chosen to be identical to the physical grid at the root of the wing in Fig. 6. It is noted here that any wing span station can be selected instead of the root for this matching. (However, numerical experiments for the F5 wing indicated that the best results can be obtained by selecting the root station.) Using Eq. (2), the physical grid on the wing is computed. It is assumed that the physical grid boundaries, far upstream and downstream, are perpendicular to the root. Then, for any given span station, physical grid points between the wing edges and the upstream and downstream boundaries are distributed in such a manner that they satisfy the three requirements mentioned in the preceding paragraph. This distribution is accomplished by employing a combination of an exponential stretching function and a coordinate smoothing function at each span station as follows.

For a given wing planform, the physical mesh on the wing surface is obtained by the transformation given by Eq. (2). From this, the grid spacing and its derivatives in the streamwise direction are computed for the mesh points adjacent to the leading and trailing edges. Next, the number of mesh points upstream of the leading edge and downstream of the trailing edge are selected. Also, the upstream and downstream boundaries of the flow region are fixed so that they are aligned with the flow as shown in Fig. 6. Based on the grid spacing and its derivatives at the leading and trailing edges of the wing, an exponential stretching function is numerically constructed by an iterative procedure such that the mesh boundaries are reached by the mesh with the selected number of mesh points. It is noted here that the amount of stretching depends on the span station location. Next, the mesh thus obtained is smoothed by the use of the heat equation. This is done in order to ensure smooth first and second derivatives for the mesh spacings, particularly near wing leading and trailing edges where two types of meshes are connected.

The transformation Eq. (2) can be rewritten as

$$\xi(x,y)=[x-x_{LE}(y)]/p(x,y), \qquad \eta(y)=y, \qquad \zeta(z)=z \tag{3}$$

where the exponential function $p(x, y)$ is numerically obtained by the procedure explained above. The preliminary results on

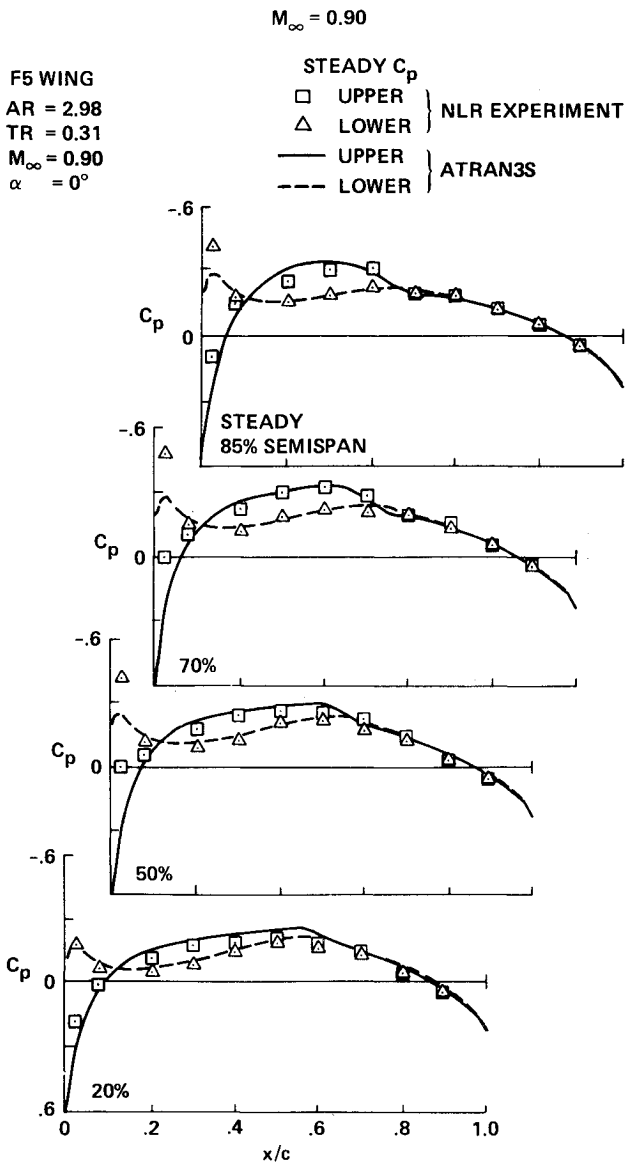

Fig. 10 Comparison of steady pressures between theory and experiment at $M = 0.90$.

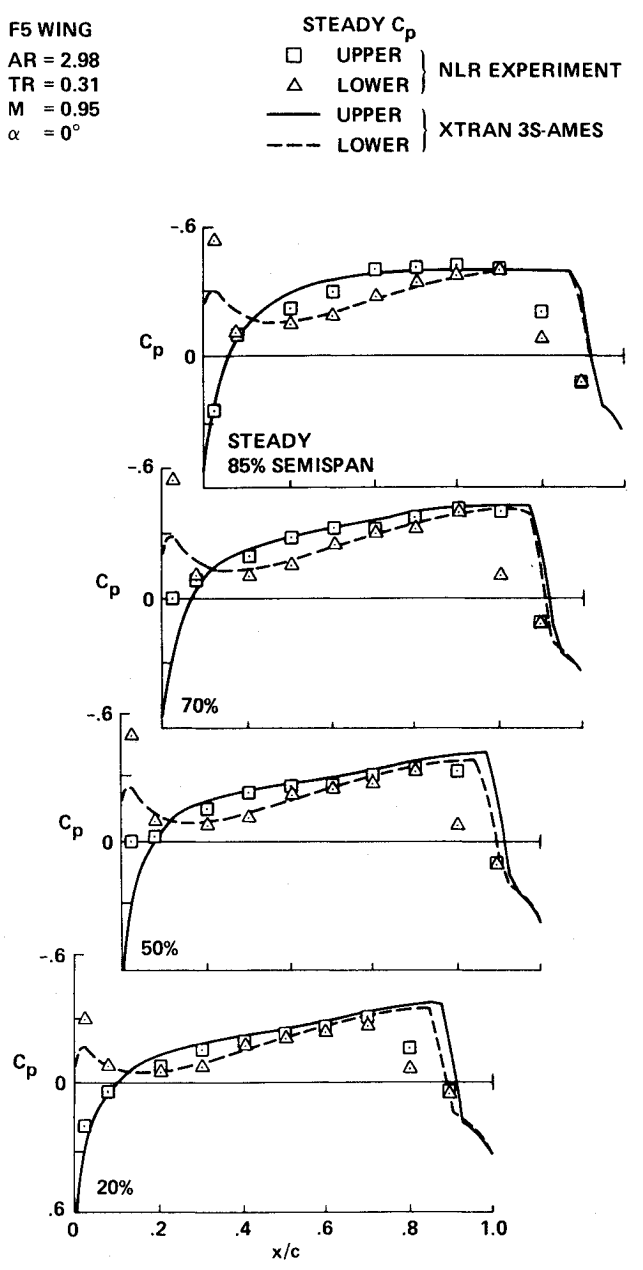

Fig. 11 Comparison of steady pressures between theory and experiment at $M = 0.95$.

this transformation were first presented by the authors in a workshop at NASA Langley.[12] Figure 6 shows the physical grid obtained by using the new procedure. The new properties of this grid can be seen by comparison with Fig. 3.

After applying the transformation, Eq. (1) can be rewritten as

$$\frac{\partial}{\partial t}\left(-\frac{A\phi_t}{\xi_x} - B\phi_\xi\right) + \frac{\partial}{\partial \xi}\left[(\xi_x E)\phi_\xi + (\xi_x^2 F)\phi_\xi^2 + G(\xi_y\phi_\xi + \phi_\eta)^2 + \frac{\xi_y}{\xi_x}(\xi_y\phi_\xi + \phi_\eta) + H\xi_y\phi_\xi(\xi_y\phi_\xi + \phi_\eta)\right] + \frac{\partial}{\partial \eta}\left[\frac{1}{\xi_x}(\xi_y\phi_\xi + \phi_\eta) + H\phi_\xi(\xi_y\phi_\xi + \phi_\eta)\right] + \frac{\partial}{\partial \zeta}\left(\frac{\phi_\zeta}{\xi_x}\right) = 0 \qquad (4)$$

It is noted here that when the conventional transformation was used to obtain Eq. (4), the ξ_x metric quantities would have been replaced by the reciprocal of the local chord. Equation (4) is solved by an ADI algorithm in XTRAN3S.[2]

Metric quantities required in Eq. (4) are computed by mapping the physical grid in Fig. 6 to the computational grid in Fig. 5. Plots of the metric quantity ξ_y vs the *chord* for the root section and vs the *span* along a grid line starting at a distance 15.6 chords from the leading edge of the root section are shown in Figs. 4a and 4b, respectively. From these two figures, the small gradients of ξ_y obtained by the modified transformation can be seen particularly in Fig. 4b at the location near the tip. It is noted that the modified transformation yields metrics ξ_x that are functions of both x and y. There is no skewness in the grid at the far-field boundaries and, hence, there is a smooth metric quantity for the finite differencing, particularly of cross derivatives. This improvement stabilizes the ADI scheme for low-taper ratio wings.

This new coordinate transformation, along with many other improvements, is incorporated in a new version of the code, XTRAN3S-Ames (ATRAN3S).[13]

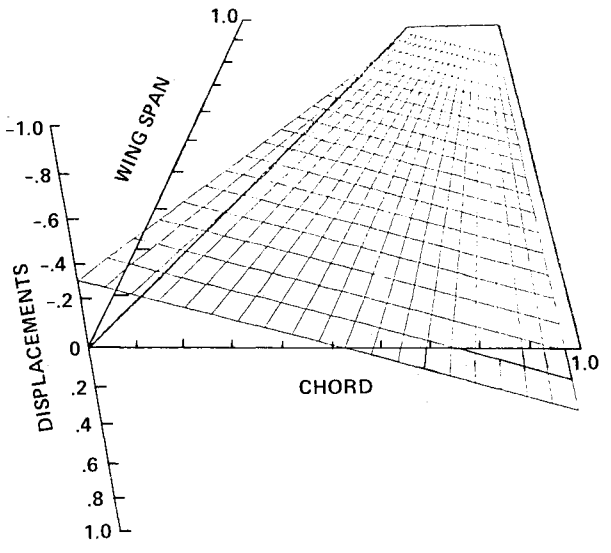

Fig. 12 Unsteady modal motion of the F5 wing.

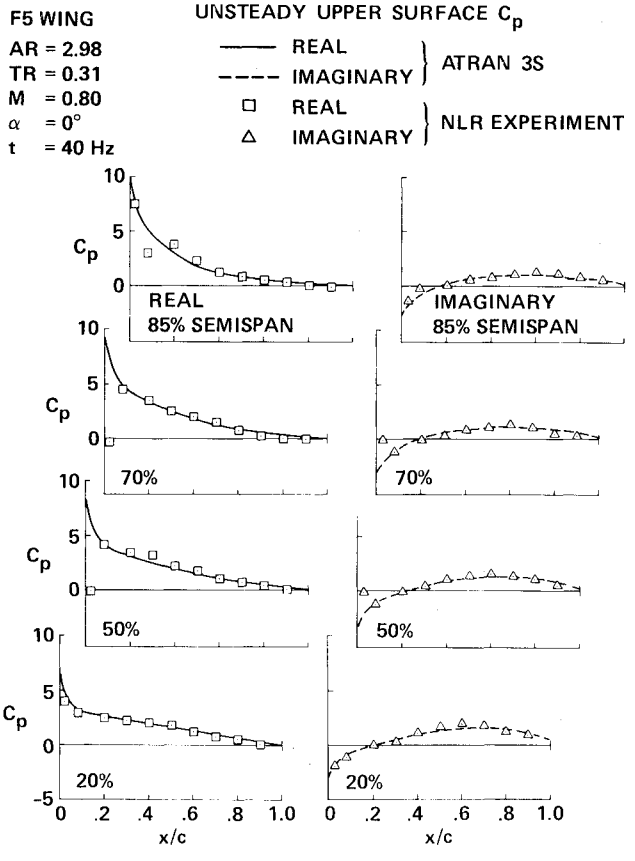

Fig. 13 Comparison of unsteady upper surface pressures between theory and experiment at $M=0.80$.

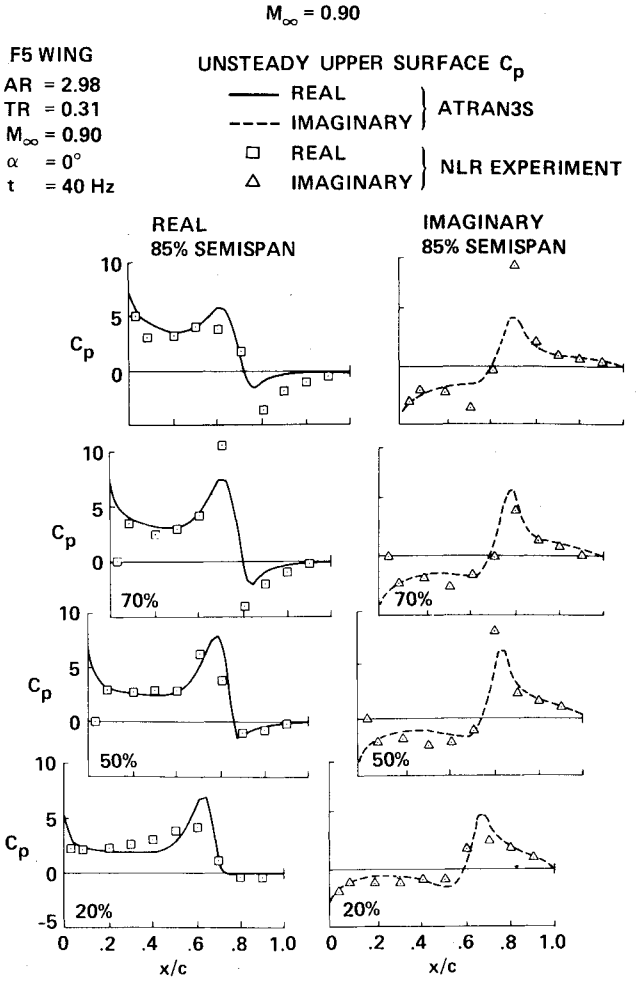

Fig. 14 Comparison of unsteady upper surface pressures between theory and experiment at $M=0.90$.

Results

Using the new transformation technique, steady and unsteady aerodynamic results are computed for the F5 wing at $M=0.80$, 0.90, and 0.95 and are compared with experimental measurements[9] and with results obtained from the conventional shearing transformation.

Figure 7 shows the plots of steady pressure results obtained for the mid-semispan station at $M=0.80$ from the two transformation methods and the experiment. With the conventional shearing transformation, about 2000 time steps of size 0.001 were required to obtain a fairly converged solution, whereas modified transformation required only about 1000 steps of size 0.01 to give a converged solution. The latter solution compares better with experiment than does the former. This illustrates that the modified shearing transformation can give more accurate results in half the computational time. Plots of steady pressure distributions obtained by the modified transformation and experiment are given for four span stations in Fig. 8. Comparisons are good at all span stations.

Figure 9 shows plots of steady pressure results obtained at $M=0.9$ for the mid-semispan station by the two transformation methods and experiment. In spite of using a time-step size of 0.001, results from the conventional shearing transformation eventually diverged. Also, those results were highly inaccurate after 4000 time steps, as illustrated in Fig. 9. The computations diverged sometime after 4000 time steps and before 6000 time steps. With the modified shearing transformation, a converged solution was obtained by using 2000 time steps of size 0.01. In Fig. 9, it can be seen that the latter method compares well with the experiment. Plots of steady pressure distributions for four span stations obtained by the modified transformation and the experiment are given in Fig. 10. Comparisons are generally good at all span stations.

Figure 11 shows the plots of steady pressure distributions obtained by the modified transformation method and the experiment at $M=0.95$. From the observations made at $M=0.90$, no attempt was made to make any computations using the conventional shearing transformation. In Fig. 11 it can be observed that the shocks given by the code are stronger and

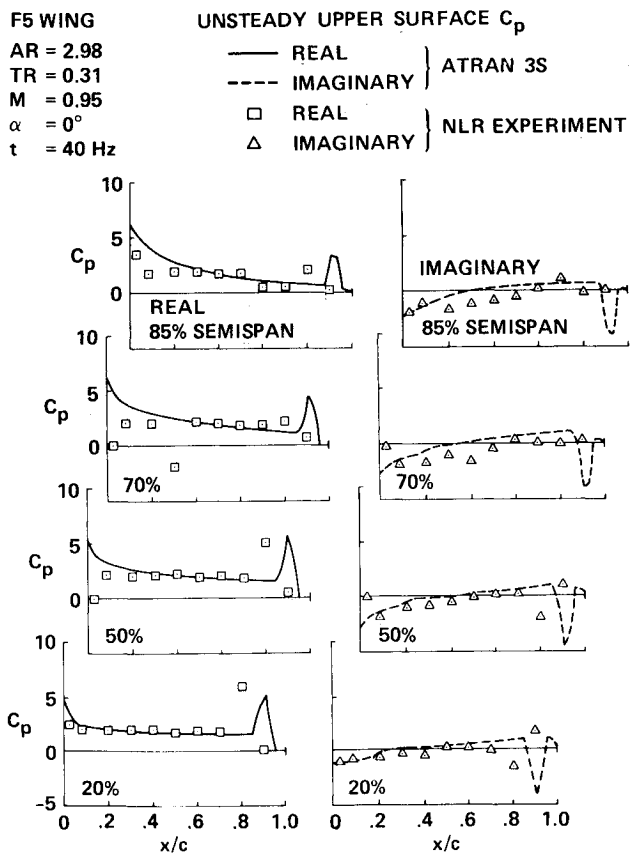

Fig. 15 Comparison of unsteady upper surface pressures between theory and experiment at $M=0.95$.

shifted farther aft as compared to those observed in the experiment. This disagreement could be due to viscous effects, since the calculations assume that the flow is inviscid. At this Mach number, viscous effects can play an important role due to the strength of the shock wave, as shown in Fig. 11.

Figure 12 shows the modal motion used in the experiment conducted at the National Aerospace Laboratory of the Netherlands (NLR).[9] The wing is pitching about an axis located at the 50% root chord, and the pitching axis is normal to the wing root. Figures 13-15 show plots of the real and imaginary values of the upper surface pressures at four span stations obtained by the modified shearing transformation and the NLR experiments at $M=0.8$, 0.9, and 0.95, respectively. These results were obtained for the wing oscillating at a frequency of 40 cycles/s.

The same modal motion used in the NLR experiment was simulated in the code. Results from the code were obtained by forcing the wing to undergo a sinusoidal modal motion for three cycles with 1200 time steps/cycle, during which time the transients disappeared and a periodic response was obtained. No attempt was made to use the conventional shearing transformation because of the instabilities encountered during the steady calculations.

As shown in Fig. 13, at $M=0.80$, where the flow is subsonic, both the real and imaginary parts of the unsteady pressure compare well with the experiment for all span stations as expected. At $M=0.90$, where the flow was transonic, as shown in Fig. 14, comparisons with the experiment are good except near the root and the tip. Discrepancies near the root can be due to the wall effects which were not accounted for in this analysis. Comparisons for span stations closer to the tip than the 85% span station were less favorable than the 85% span station. A better agreement near the tip might be obtained through the use of more computational span stations in that region. At $M=0.95$, comparisons with the experiment are not as favorable as at the lower Mach numbers. As seen in Fig. 15, this disagreement with the NLR experiment is mainly in the region of shock wave. The results could be improved if viscous corrections were applied to the calculations. The code ATRAN3S is now capable of making such viscous corrections.[14] Comparisons similar to those obtained for the upper surface were also obtained for the lower surface pressure distributions.

Concluding Remarks

An efficient, modified shearing-transformation method has been developed for use in the code ATRAN3S, which computes unsteady transonic aerodynamics. This new method is particularly effective for low-aspect ratio and small-taper ratio delta-type wings. From the computations made on the F5 wing and subsequent comparisons with experiment, it can be concluded that the modified transformation makes the finite-difference scheme used in ATRAN3S accurate, stable, and fast for these difficult cases. Cases can now be successfully analyzed for which the conventional shearing transformation had failed to yield results. Computations made with this new procedure demonstrate that the range of the unsteady transonic code ATRAN3S for aerodynamic and aeroelastic applications has been extended.

References

[1]Ballhaus, W. F., Deiwert, G. S., Goorjian, P. M., Holst, T. L., and Kutler, P., "Advances and Opportunities in Transonic Flow Computations," *Numerical and Physical Aspects of Aerodynamic Flows*, Springer-Verlag, New York, 1981.

[2]Borland, C. J. and Rizetta, D. P., "Transonic Unsteady Aerodynamics for Aeroelastic Applications, Vol. I—Technical Development Summary for XTRAN3S," AFWAL-TR-80-3107, June 1982.

[3]Traci, R. M., Albano, E. D., and Farr, J. L., "Small Disturbance Transonic Flows About Oscillating Airfoils and Planar Wings," AFFDL-TR-75-100, Air Force Flight Dynamics Laboratory, June 1975.

[4]Sankar, N. L., Malone, J. B., and Tassa, Y., "An Implicit Conservative Algorithm for Steady and Unsteady Three-Dimensional Transonic Potential Flows," AIAA Paper 81-1016, June 1981.

[5]Borland, C. J. and Rizetta, D. P., "Nonlinear Transonic Flutter Analysis," AIAA Paper 81-0608-CP, April 1981.

[6]Guruswamy, P. and Goorjian, P. M., "Comparison Between Computational and Experimental Data in Unsteady Three Dimensional Transonic Aerodynamics Including Aeroelastic Applications," AIAA Paper 82-0690-CP, May 1982; see also *Journal of Aircraft*, Vol. 21, Jan. 1984, pp. 37-43.

[7]Myers, M. R., Guruswamy, P., and Goorjian, P. M., "Flutter Analysis of a Transport Wing Using XTRAN3S," AIAA Paper 83-0922, May 1983.

[8]Seidel, D. A., Bennett, R. M., and Ricketts, R. H., "Some Applications of XTRAN3S," NASA TM-85641, May 1983.

[9]Tijdeman, J. et al., "Transonic Wind Tunnel Tests on an Oscillating Wing with External Stores; Part II—The Clean Wing," AFFDL-TR-78-194, March 1979.

[10]Yoshihara, H., "Formulation of the Three-Dimensional Transonic Unsteady Aerodynamic Problem," AFFDL TR-79-3030, Feb. 1979.

[11]Ballhaus, W. F. and Bailey, F. R., "Numerical Calculation of Transonic Flow About Swept Wings," AIAA Paper 72-677, June 1972.

[12]Goorjian, P. M. and Guruswamy, P., "Unsteady Transonics," Transonic Unsteady Aerodynamics and Aeroelasticity Workshop, NASA Langley Research Center, June 1983.

[13]Guruswamy, P. and Goorjian, P. M., "Development and Applications of XTRAN3S-Ames," Computational Fluid Dynamics User's Workshop, The University of Tennessee Space Institute, Tullahoma, Tenn., March 1984.

[14]Rizzetta, D. P. and Borland, C. J., "Numerical Solution of Three-Dimensional Unsteady Transonic Flow Over Wings, Including Inviscid/Viscous Interaction," AIAA Paper 82-0352, Jan. 1982.